

**RADIATION AND MASS TRANSFER EFFECTS ON MHD FLOW OF AN ELASTO-VISCOUS FLUID IN AN INFINITE VERTICAL PLATE: FINITE DIFFERENCE METHOD**

**D. RAJU\***

**Department of Mathematics,  
Vidya Jyothi Institute of Technology (A),  
Aziz Nagar Gate, C. B. Post, Hyderabad, Telangana-500 075.**

*(Received On: 14-10-17; Revised & Accepted On: 09-11-17)*

---

**ABSTRACT**

*This paper is focused on the effects of radiation and mass transfer on a unsteady free convective viscoelastic fluid flow of incompressible, electrically conducting and chemically reacting fluid past an impulsively started moving vertical plate adjacent to Darcian porous regime in the presence of heat generation. The plate temperature is raised linearly with time  $t$  and the concentration level near the plate is raised to  $C'_w$ . The governing boundary-layer equations are formulated in an  $(y, t)$  coordinate system with appropriate boundary conditions. The Rosseland diffusion approximation is used to analyze the radiative heat flux in the energy equation, which is appropriate for non-scattering media. The dimensionless governing equations are solved using Crank Nicolson finite difference technique. A parametric study is performed to illustrate the influence of thermophysical parameters on the velocity, temperature and concentration profiles. Also, the local and average skin-friction, Nusselt number and Sherwood number are presented graphically*

**Keywords:** Radiation, Mass transfer, MHD, Free convection, Mass diffusion, Visco-elastic fluid, Porous medium, Heat source.

---

**INTRODUCTION**

In reality, most of the fluids considered in industrial applications are more Non-Newtonian in nature, especially of viscoelastic type than viscous type. And also, there may be a situation of a heat source/sink present in the boundary layer. The investigation of heat transfer processes plays an important role in all such theoretical studies. This is due to the fact that a number of metallurgical processes in a polymer processing industry involve the cooling of continuous sheet or filament. The rate of cooling influences a lot the quality of the final product with desired characteristics. The flow and heat transfer characteristics of a copper–water nanofluid was studied experimentally by Li and. Xuan [9]. Microencapsulated phase change slurries were studied in circular tubes with constant heat flux analysed by Hu and Zhang [10]. Forced convective heat transfer augmentation was considered for the addition of metallic fibrous materials studies by Angirasa [11]. Barbosa *et.al* [12] studied Adiabatic air–water experiments were conducted to address the transition regime between churn and annular flow. Heat transfer coefficients were determined for fluid-to-particle continuous flow of suspensions in coiled tube and straight tubes with bends by Chakrabandhu and Singh [13]. A LiBr–water absorber was modeled; falling-film and droplet mode heat transfer was addressed by Jeong and Garimella [14]. Six different two-phase non-boiling heat transfer correlations were assessed using extensive data sets by Kim [15]. Heat transfer measurements were also used to develop correlations for air–water flow in horizontal pipes by Kim and Ghajar [16]. Experimental heat transfer coefficients were obtained for a vertical tube positioned at various locations in a circulating fluidized bed by Kolar and Sundaresan [17]. A perturbation-based stochastic finite element method was used to obtain the heat transfer of a viscoelastic fluid containing elastic spherical particles by Kaminski [18]. Nusselt numbers were predicted for power-law fluids in ducts of various cross-sectional areas; rhombic, isosceles-triangular, elliptical, and semielliptical ducts were considered Syrjala [19]. A Bingham fluid in a thermal entry region was studied using a finite integral transform technique by Nascimento [20]. The effects of power-law rheology, duct eccentricity and thermal boundary conditions were considered in fully developed laminar flow Manglik and Fang [21]. Power-law laminar flow was also addressed in a conjugate heat transfer problem in a circular tube by Luna *et.al* [22]. Fully-developed laminar flow of a Phan–Thien– Tanner fluid was examined in pipes and channels with constant wall temperature by Coelho *et.al* [23].

---

**Corresponding Author: D. Raju\***

**Department of Mathematics, Vidya Jyothi Institute of Technology (A),  
Aziz Nagar Gate, C. B. Post, Hyderabad, Telangana-500 075.**

The hydromagnetic convection with heat and mass transfer in porous medium has been studied due to its importance in the design of MHD generators and accelerators in geophysics, in design of underground water energy storage system, soil–sciences, astrophysics, nuclear power reactors and so on. Magneto hydrodynamics is currently undergoing a period of great enlargement and differentiation of subject matter. The interest in these new problems generates from their importance in liquid metals, electrolytes and ionized gases. Heat transfer in the transition region to rarefied gas flow was analyzed with Grads moment method, the Boltzmann equation and a linearized collision term by Struchtrup [24]. Important to the problem was describing the boundary condition for the moments. Gas flow over microscale airfoils was numerically simulated using both particle and continuum approaches Sun *et.al* [25]. The continuum approach was considered to not be suitable for the flow under study due to rarefied effects. Computation of the Chapman–Enskog functions for viscosity and heat transfer in Poiseuille flow was discussed by Siewert [26]. Direct methods for exact solutions of hydrodynamic and heat and mass transfer equations by the generalized and functional separation of variables were proposed by Polyanin and Zhurov [27].

The effects of radiation on unsteady free convection flow and heat transfer problem have become more important industrially. At high operating temperature, radiation effect can be quite significant. Many processes in engineering areas occur at high temperature and knowledge of radiation heat transfer becomes very important for design of reliable equipments, nuclear plants, gas turbines and various propulsion devices or aircraft, missiles, satellites and space vehicles. Thus thermal radiation is one of the vital factors controlling the heat and mass transfer. Pal and Mondal, [28] Influence of temperature-dependent viscosity and thermal radiation on MHD forced convection over a non-isothermal wedge. Ram *et.al* [29] Effect of magnetic field-dependent viscosity on revolving ferro fluid. Hossain and Pop, [30] Radiation effect on Darcy free convection in boundary layer flow along an inclined surface placed in porous media.

The distribution of solute undergoing chemical reaction corresponding to boundary layer flow due to moving sheet are relevant to many practical applications in the metallurgy industry, filaments drawn through a quiescent electrically conducting fluid and the purification of molten metal's from non-metallic inclusions. In these situations, the boundary layer flow consideration is appropriate to understand the processes. Muthucumaraswamy and Ganesan [5] studied effect of the chemical reaction and injection on flow characteristics in an unsteady upward motion of an isothermal plate. Deka *et.al* [2] studied the effect of the first order homogeneous chemical reaction on the process of an unsteady flow past an infinite vertical plate with a constant heat and mass transfer. Soundalgekar and Patti [7] studied the problem of the flow past an impulsively started isothermal infinite vertical plate with mass transfer effects. Chamkha [1] assumed that the plate is embedded in a uniform porous medium and moves with a constant velocity in the flow direction in the presence of a transverse magnetic field. Raptis [6] investigate the steady flow of a viscous fluid through a porous medium bounded by a porous plate subjected to a constant suction velocity by the presence of thermal radiation. Effects of the chemical reaction and radiation absorption on free convection flow through porous medium with variable suction in the presence of uniform magnetic field were studied by Sudheer Babu and Satyanarayana [8]. Kesavaiah *et.al* [4] effects of the chemical reaction and radiation absorption on an unsteady MHD convective heat and mass transfer flow past a semi-infinite vertical permeable moving plate embedded in a porous medium with heat source and suction. Gireesh Kumar and Satyanarayana [3] Mass transfer effects on MHD unsteady free convective Walter's memory flow with constant suction and heat sink.

However, the interaction of radiation with mass transfer in a chemically reacting and electrically conducting visco-elastic fluid past an impulsively started plate embedded in a Darcy porous medium in the presence of heat generation has received little attention. Hence, the present study is attempted. Such study has significant applications in solar collection systems, fire dynamics in insulations, and also geothermal energy systems. The volumetric heat generation term may exert a strong influence on the heat transfer and as a consequence, also on the fluid flow. The transformed problem is shown to be dictated by the thermo physical and hydrodynamic parameters, viz., dimensionless time, thermal Grashof number, species Grashof number, magnetic parameter, Darcy number, Reynolds number, Prandtl number, heat generation parameter, radiation parameter and Schmidt number. The influence of these parameters on the velocity profiles, temperature function, mass transfer function, local and average shear stresses, local and average Nusselt numbers and local and average Sherwood numbers are presented and discussed at length.

## FORMULATION AND SOLUTION OF THE PROBLEM

The unsteady free convection and mass transfer flow of an electrically conducting incompressible elasto-viscous fluid past an infinite vertical plate through porous medium in the presence of radiating heat source in the presence of chemical reaction has been considered. A magnetic field of uniform strength  $B_0$  is applied transversely to the plate. The induced magnetic field is neglected as the magnetic Reynolds number of the flow is taken to be very small. The flow is assumed to be in  $x$  – direction which is taken along the vertical plate in the upward direction. The  $y$  – axis is taken to be normal to the plate. Initially the plate and the fluid are at the same temperature  $T'$  with concentration level  $C'_\infty$  at all points. At time  $t' > 0$ , the plate is exponentially accelerated with a velocity  $u = \varepsilon(\exp a't')$  in its own plane and the plate temperature is raised linearly with time  $t$  and the level of concentration near the plate is raised to  $C'_w$ . The effect of viscous dissipation is assumed to be negligible. Then by usual Boussinesq's approximation, the unsteady flow is governed by the following equations.

$$\frac{\partial u'}{\partial t'} = g\beta(T' - T'_\infty) + g\beta^*(C' - C'_\infty) + \nu \frac{\partial^2 u'}{\partial y'^2} - \frac{K_0}{\rho} \left( \frac{\partial^3 u'}{\partial y'^2 \partial t'} \right) - \frac{\nu}{K'} u' - \frac{\sigma B_0^2}{\rho} u' \tag{1}$$

$$\rho C_p \frac{\partial T'}{\partial t'} = K \frac{\partial^2 T'}{\partial y'^2} - \frac{\partial q_r}{\partial y'} + Q' \tag{2}$$

$$\frac{\partial C'}{\partial t'} = D \frac{\partial^2 C'}{\partial y'^2} - Kr'(C' - C'_\infty) \tag{3}$$

The initial and boundary conditions for the velocity, temperature and concentration fields are

$$\begin{aligned} u' = 0, T' = T'_\infty, C' = C'_\infty & \quad \text{for all } y', t' \leq 0 \\ u' = \varepsilon \exp(a't'), T' \rightarrow T'_\infty + (T'_w - T'_\infty)At', C' = C'_\infty, t' > 0 & \quad \text{at } y' = 0 \\ u' = 0, T' \rightarrow T'_\infty, C' \rightarrow C'_\infty & \quad \text{as } y' \rightarrow \infty \end{aligned} \tag{4}$$

Where  $u'$  is the velocity of the fluid along the plate in the  $x'$  - direction,  $t'$  is the time,  $g$  is the acceleration due to gravity,  $\beta$  is the coefficient of volume expansion,  $\beta^*$  is the coefficient of thermal expansion with concentration,  $T'_\infty$  is the temperature of the fluid near the plate,  $T'_w$  is the temperature of the fluid far away from the plate,  $T'_w$  is the temperature of the fluid,  $C'$  is the species concentration in the fluid near the plate,  $C'_\infty$  is the species concentration in the fluid far away from the plate,  $\nu$  is the kinematic viscosity,  $K_0$  is the coefficient of kinematic visco-elastic parameter,  $\sigma$  is the electrical conductivity of the fluid,  $B_0$  is the strength of applied magnetic field,  $\rho$  is the density of the fluid,  $C_p$  is the specific heat at constant pressure,  $K$  is the thermal conductivity of the fluid,  $\mu$  is the viscosity of the fluid,  $D$  is the molecular diffusivity,  $u_0$  is the velocity of the plate.

The radiative heat flux  $q_r$  is given by equation (5) in the spirit of Cogley *et.al* [31]

$$\frac{\partial q_r}{\partial y'} = 4(T' - T'_\infty)I \tag{5}$$

where  $I = \int_0^\infty K_{\lambda w} \frac{\partial e_{b\lambda}}{\partial T^*} d\lambda$ ,  $K_{\lambda w}$  is the absorption coefficient at the wall and  $e_{b\lambda}$  is Planck's function,  $I$  is absorption coefficient

Equations (1) - (3) can be made dimensionless by introducing the following dimensionless variables and parameters:

In order to write the governing equations and the boundary conditions in dimensionless form, the following non-dimensional quantities are introduced.

$$\begin{aligned} u = \frac{u'}{u_0}, y = \frac{u_0 y'}{\nu}, t = \frac{t' u_0^2}{\nu}, \theta = \frac{T' - T'_\infty}{T'_w - T'_\infty}, K = \frac{K' u_0^2}{\nu^2}, Kr = \frac{Kr' \nu}{U_0^2} \\ C = \frac{C' - C'_\infty}{C'_w - C'_\infty}, Pr = \frac{\mu C_p}{\kappa}, Sc = \frac{\nu}{D}, Q = \frac{\nu Q'}{\rho C_p u_0^2}, S = \frac{K_0 u_0^2}{\rho \nu^2}, a = \frac{a' \nu}{u_0^2} \\ M = \frac{\sigma B_0^2 \nu}{\rho u_0^2}, Gr = \frac{\nu \beta g (T'_w - T'_\infty)}{u_0^3}, Gm = \frac{\nu \beta^* g (C'_w - C'_\infty)}{u_0^3}, R = \frac{4\nu I}{\rho C_p u_0^2} \end{aligned} \tag{6}$$

where  $Gr$  is the thermal Grashof number,  $Gc$  is modified Grashof Number,  $Pr$  is Prandtl Number,  $M$  is the magnetic field,  $R$  is the radiation parameter,  $Sc$  is Schmidt number,  $Kr$  is Chemical Reaction,  $K$  is Porous Permeability,  $Q$  is Heat source parameter respectively.

In terms of the above dimensionless quantities, Equations (1) - (2) reduces to

$$\frac{\partial u}{\partial t} = Gr \theta + Gm C + \frac{\partial^2 u}{\partial y^2} - S \left( \frac{\partial^3 u}{\partial y^2 \partial t} \right) - M u - \frac{1}{K} u \tag{7}$$

$$\text{Pr} \frac{\partial \theta}{\partial t} = \frac{\partial^2 \theta}{\partial y^2} - R \text{Pr} \theta + Q \text{Pr} \theta \tag{8}$$

$$\text{Sc} \frac{\partial C}{\partial t} = \frac{\partial^2 C}{\partial y^2} - Kr \text{Sc} C \tag{9}$$

The corresponding boundary conditions are

$$\begin{aligned} u = 0, \theta = 0, C = 0 \quad t \leq 0 \quad \text{for all } y \\ u = \exp(at), \theta = 1, C = 1, t > 0 \quad \text{at } y = 0 \\ u = 0, \theta \rightarrow 0, C \rightarrow 0 \quad \text{as } y \rightarrow \infty \end{aligned} \tag{10}$$

In the present analysis we have considered the heat generation (absorption) of the type

$$Q' = Q_0 (T' - T'_\infty)$$

Where  $\frac{Q'}{\rho C_p}$  is the volumetric rate of heat generation (absorption). For solving the problem, we take, Beard and

Walters [32], u in the form

$$u = U_o + SU_1$$

### SOLUTION OF THE PROBLEM

Equation (7) – (9) are coupled, non – linear partial differential equations and these cannot be solved in closed – form using the initial and boundary conditions (10). However, these equations can be reduced to a set of ordinary differential equations, which can be solved analytically. This can be done by representing the velocity, temperature and concentration of the fluid in the neighbourhood of the fluid in the neighbourhood of the plate as

$$\begin{aligned} \left[ \frac{u_{i,j+1} - u_{i,j}}{\Delta t} \right] = Gr \left[ \theta_{i,j} \right] + Gc \left[ C_{i,j} \right] + \left[ \frac{u_{i-1,j} - 2u_{i,j} + u_{i+1,j}}{(\Delta y)^2} \right] \\ - S \left[ \frac{u_{i-1,j+1} - 2u_{i,j+1} + u_{i+1,j+1} - u_{i-1,j} + 2u_{i,j} - u_{i+1,j}}{\Delta t. (\Delta y)^2} \right] - M \left[ u_{i,j} \right] - \frac{1}{K} \left[ u_{i,j} \right] \end{aligned} \tag{11}$$

$$\text{Pr} \left[ \frac{\theta_{i,j+1} - \theta_{i,j}}{\Delta t} \right] = \left[ \frac{\theta_{i-1,j} - 2\theta_{i,j} + \theta_{i+1,j}}{(\Delta y)^2} \right] - R \text{Pr} \left[ \theta_{i,j} \right] + Q \text{Pr} \left[ \theta_{i,j} \right] \tag{12}$$

$$\text{Sc} \left[ \frac{C_{i,j+1} - C_{i,j}}{\Delta t} \right] = \left[ \frac{C_{i-1,j} - 2C_{i,j} + C_{i+1,j}}{(\Delta y)^2} \right] - Kr \text{Sc} \left[ C_{i,j} \right] \tag{13}$$

Here, index i refer to y and j to time. The mesh system is divided by taking  $\Delta y = 0.1$ .

From the initial condition in (9), we have the following equivalent:

$$u(i, 0) = 0, \theta(i, 0) = 0, C(i, 0) = 0 \quad \text{for all } i \tag{14}$$

The boundary conditions from (9) are expressed in finite-difference form as follows

$$\begin{aligned} u(0, j) = 1, \theta(0, j) = 1, C_{i-1,j} - C_{i+1,j} = -2 \quad \text{for all } j \\ u(i_{\max}, j) = 0, \theta(i_{\max}, j) = 0, C(i_{\max}, j) = 0 \quad \text{for all } j \end{aligned} \tag{15}$$

Here  $i_{\max}$  was taken as 50

First the velocity at the end of time step viz  $u(i, j+1)$  ( $i=1, 50$ ) is computed from (11) in terms of velocity, temperature and concentration at points on the earlier time-step. Then  $\theta(i, j+1)$  is computed from (11) and  $C(i, j+1)$  is computed from (13). The procedure is repeated until  $t = 0.5$  (i.e.  $j = 500$ ). During computation  $\Delta t$  was chosen as 0.001.

To judge the accuracy of the convergence and stability of finite difference scheme, the same program was run with different values of  $\Delta t$  i.e.,  $\Delta t = 0.0009, 0.0001$  and no significant change was observed. Hence, we conclude that the finite-difference scheme is stable and convergent.

**Skin-friction:**

We now calculate Skin-friction from the velocity field. It is given in non-dimensional form as:

$$\tau = -\left(\frac{\partial u}{\partial y}\right)_{y=0}, \text{ where } \tau = -\frac{\tau'}{\rho U_0^2}$$

**Rate of heat transfer:**

The dimensionless rate of heat transfer is given by

$$Nu = -\left(\frac{\partial \theta}{\partial y}\right)_{y=0}$$

**Sherwood number:**

The dimensionless Sherwood number is given by

$$Sh = -\left(\frac{\partial C}{\partial y}\right)_{y=0}$$

**RESULTS AND DISCUSSION**

In order to get the physical insight into the problem, we have plotted velocity profiles for different parameters  $M$  (Magnetic parameter),  $K$  (permeability parameter),  $S$  (visco-elastic parameter),  $Gm$  (Mass Grashof number),  $t$  (time),  $a$  (accelerating parameter),  $Q$  (Heat source parameter),  $R$  (Radiation parameter),  $Kr$  (Chemical reaction parameter) and  $Sc$  (Schmidt number) in figures (1) to (18) for the cases of heating ( $Gr < 0$ ) and cooling ( $Gr > 0$ ) of the plate. The heating and cooling take place by setting up free convection current due to temperature and concentration gradient. This enables us to carry out the numerical calculations for the distribution of the velocity, temperature and concentration across the boundary layer for various values of the parameters. In the present study we have chosen  $\varepsilon = 0.02$ .

Figures (1) and (2) illustrate the influences of magnetic parameter ( $M$ ) on the velocity field in cases of cooling and heating of the plate at  $t = 0.2$  respectively. From these figures the velocity is found to decrease with an increase in  $M$  for the case of heating of the plate. It is because that the application of transverse magnetic field will result a resistive type force (Lorentz force) similar to drag force, which tends to resist the fluid flow and thus reducing its velocity. But the reverse effect is found in the case of cooling of the plate. It is also found that in the case of cooling, the velocity increases near the surface of the plate and becomes maximum and then decreases away from the plate. The reverse phenomenon is found in the case of heating of the plate.

Figures (3) and (4) represent the velocity profiles due to the variations in permeability parameter ( $K$ ) in cases of cooling and heating of the plate at  $t = 0.2$  respectively. From these figures the velocity is observed to increase with an increase in permeability parameter ( $K$ ) for the case of heating of the plate. This is due to the fact that the presence of a porous medium increases the resistance to flow. But the reverse effect is observed in the case of cooling of the plate.

Figures (5) and (6) display the effects of viscoelastic parameter ( $S$ ) on the velocity field for the cases cooling and heating of the plate at  $t = 0.2$  respectively. In the case of cooling of the plate, it is observed that the velocity is less for Newtonian fluid ( $S$  is equal to zero) than the Non-Newtonian fluid ( $S$  is not equal to zero) and also the velocity increases with an increase in  $S$ . But the opposite phenomenon is observed in the case of heating of the plate.

Figures (7) and (8) reveal velocity variations with mass Grashof number ( $Gm$ ) in the cases of cooling and heating of the plate at  $t = 0.2$  respectively. From the figures it is observed that the velocity increases with an increase in mass Grashof number ( $Gm$ ) in the case of cooling of the plate. It is due to the fact increase in the values of mass Grashof number has the tendency to increase the mass buoyancy effect. This gives rise to an increase in the induced flow. The reverse effect is observed in the case of heating of the plate.

Figure (9) represents the velocity profiles for different values of time ( $t$ ) in cases of heating of the plate respectively. From the figure, in the case of heating of the plate, the velocity is found to decrease with an increase in time ( $t$ ).

Figures (10) and (11) represent the velocity profiles for different values of accelerating parameter ( $a$ ) in cases of cooling and heating of the plate at  $t = 0.2$  respectively. From the figures the velocity is found to increase with an increase in accelerating parameter ( $a$ ) in cases of both cooling and heating of the plate. It is also found that the fluid velocity due to the impulsive start of the plate ( $a$  is equal to zero) is less than due to the exponentially accelerated start ( $a$  is not equal to zero) in cases of both cooling and heating of the plate.

To observe the effect of heat source parameter ( $Q$ ), the velocity profiles for different  $Q$  are presented in figures (12) and (13) in cases of cooling and heating of the plate at  $t = 0.2$  respectively. In the case of cooling of the plate, the velocity increases near the surface of the plate and becomes maximum and then decreases away from the plate. But the opposite effect is observed in the case of heating of the plate.

Figures (14) and (15) display the effects of  $Sc$  (Schmidt number) on the velocity field for the cases of cooling and heating of the plate at  $t = 0.2$  respectively. From the figures, in the case of cooling of the plate, it is found that the velocity increases with an increase in  $Sc$ . But the reverse effect is found in the case of heating of the plate.

Figure (16) and (17) illustrates the velocity profiles for the different values of radiation parameter ( $R$ ). Figure (16) we observe that the velocity decreases with increasing values of  $R$ . But figure in (17) at a particular value of  $R$ , the velocity and the thermal boundary layer thickness increase by increasing the angle of inclination, with an accompanying decrease in the wall velocity gradient. This is because of the reduction in the buoyancy force as the plate is inclined from the vertical to a large angular position.

The effects of radiation parameter ( $R$ ) on the temperature profiles are presented in figure (18). From this figure we observe that, as the value of  $R$  increases the temperature profiles decrease, with an increasing in the thermal boundary layer thickness. Figure (19) shows the variation of temperature profiles for different values of  $Q$ . It is seen from this figure that temperature profiles increase with an increasing of heat generation parameter ( $Q$ ). Typical variation of the temperature profiles along the spanwise coordinate  $y$  are shown in figure (20) for different values of Prandtl number ( $Pr$ ). The results show that an increase of Prandtl number results in a increasing the thermal boundary layer thickness and more uniform temperature distribution across the boundary layer. The reason is that smaller values of  $Pr$  are equivalent to increasing the thermal conductivities, and therefore, heat is able to differ away from the heated surface more rapidly than for higher values of  $Pr$ . Hence, the boundary layer is thicker and the rate of heat transfer is reduced, for gradient have been reduced. For different values of the chemical reaction parameter ( $Kr$ ), the concentration profiles plotted in figure (21). It is obvious that the influence of increasing values of  $Kr$ , the concentration distribution across the boundary layer decreases. Figure (22) shows the concentration profiles across the boundary layer for various values of Schmidt number ( $Sc$ ). The figure shows that an increasing in  $Sc$  results in a decreasing the concentration distribution, because the smaller values of  $Sc$  are equivalent to increasing the chemical molecular diffusivity.

FIGURES:

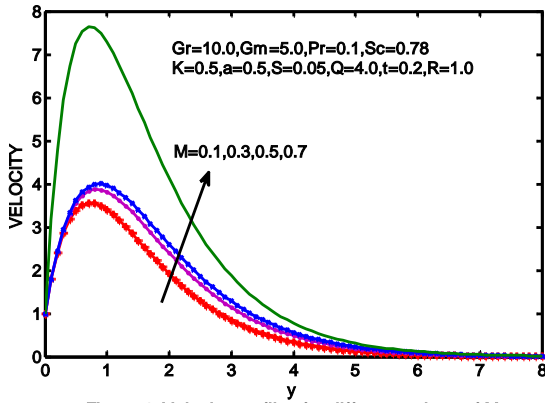


Figure 1. Velocity profiles for different values of M

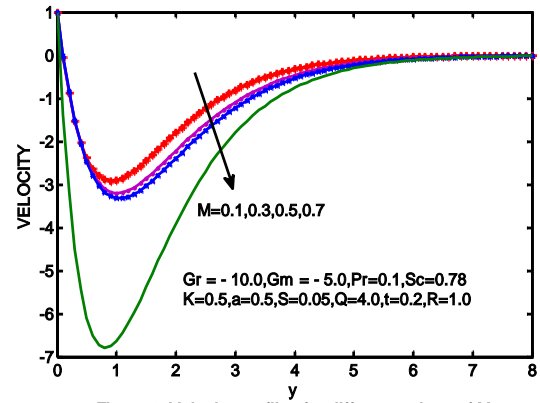


Figure 2. Velocity profiles for different values of M

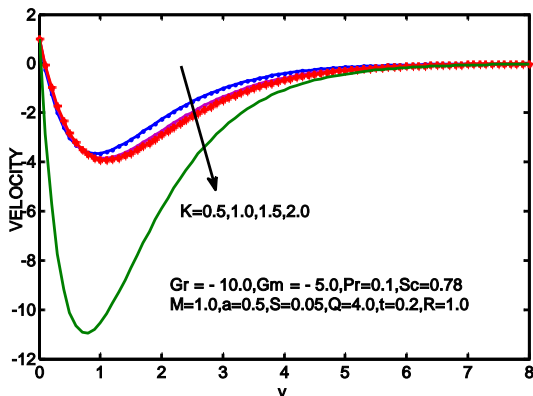


Figure 4. Velocity profiles for different values of K

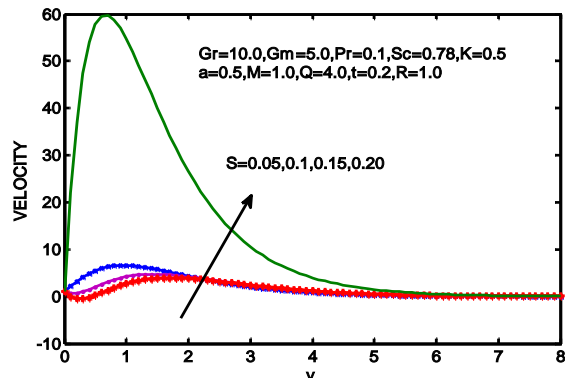


Figure 5. Velocity profiles for different values of S

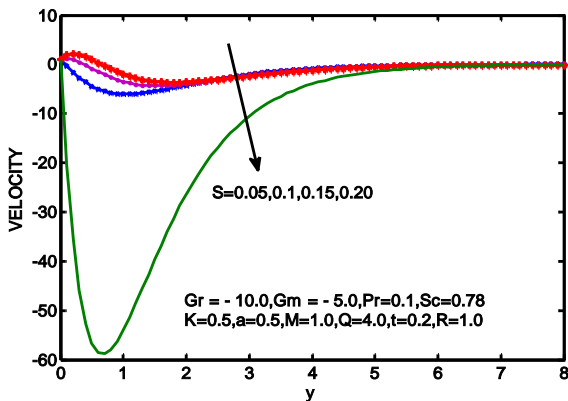


Figure 6. Velocity profiles for different values of S

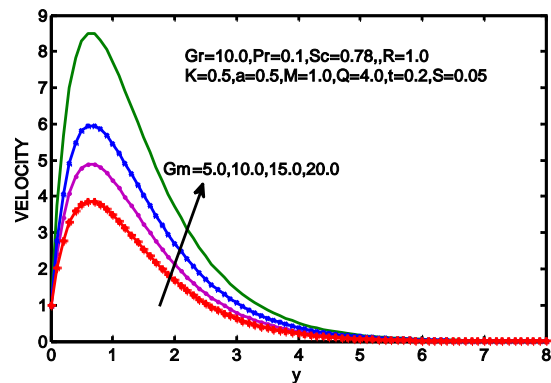


Figure 7. Velocity profiles for different values of Gm

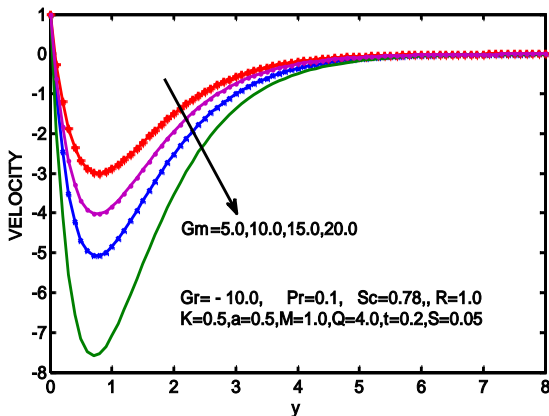


Figure 8. Velocity profiles for different values of Gm

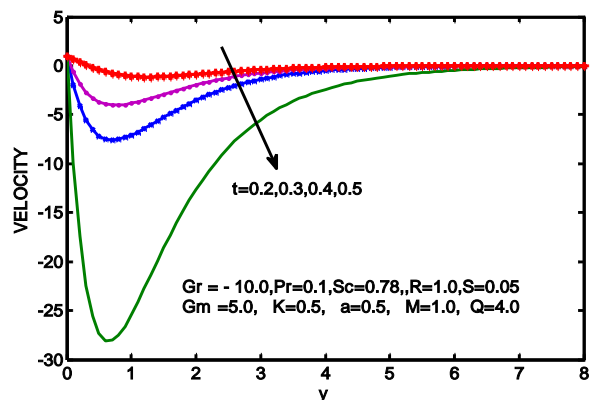


Figure 9. Velocity profiles for different values of t

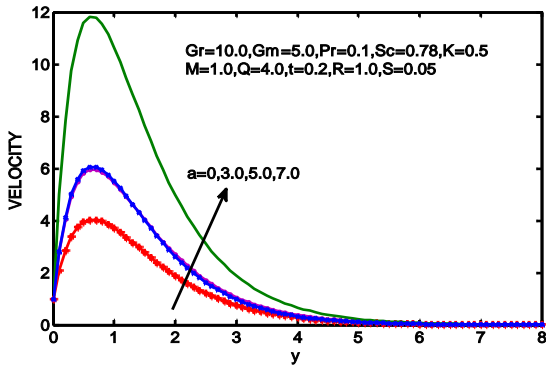


Figure 10. Velocity profiles for different values of a

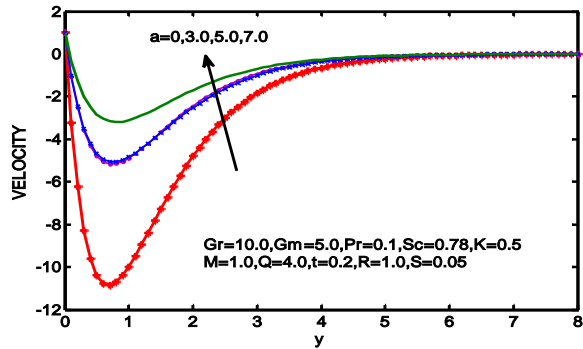


Figure 11. Velocity profiles for different values of a

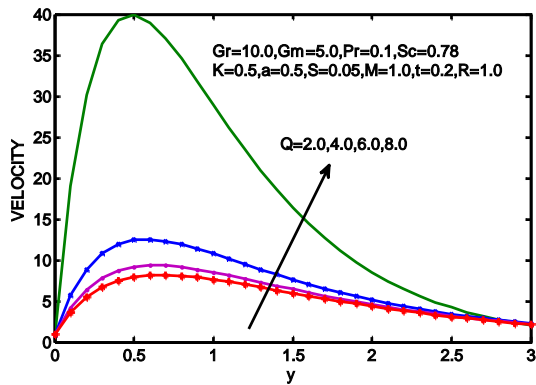


Figure 12. Velocity profiles for different values of Q

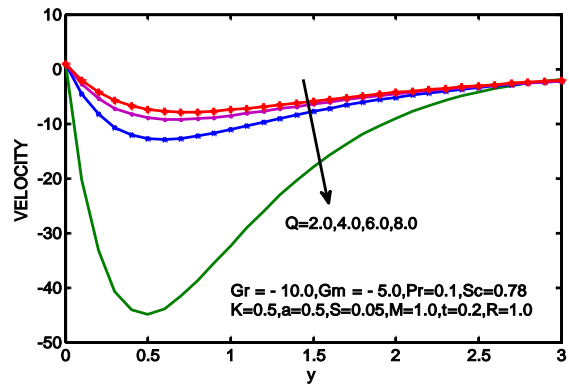


Figure 13. Velocity profiles for different values of Q

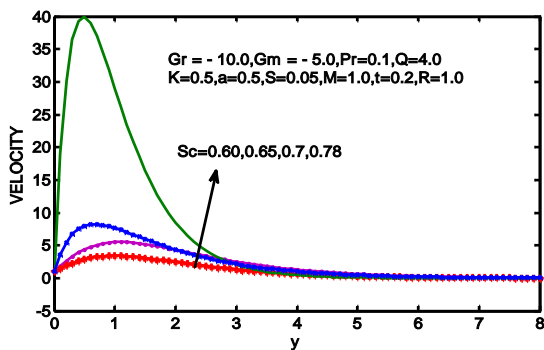


Figure 14. Velocity profiles for different values of Sc

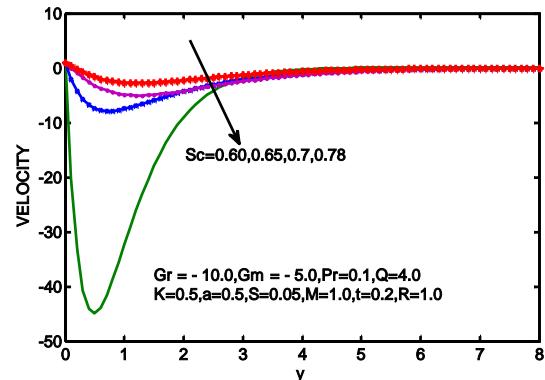


Figure 15. Velocity profiles for different values of Sc

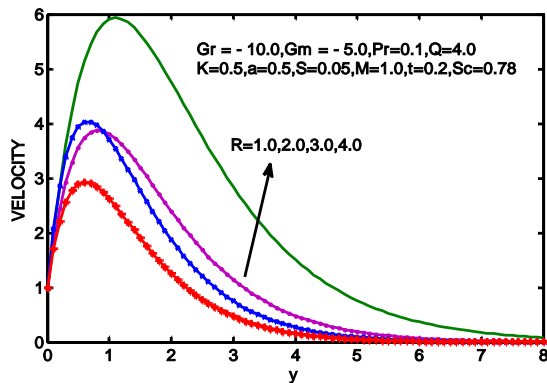


Figure 16. Velocity profiles for different values of R

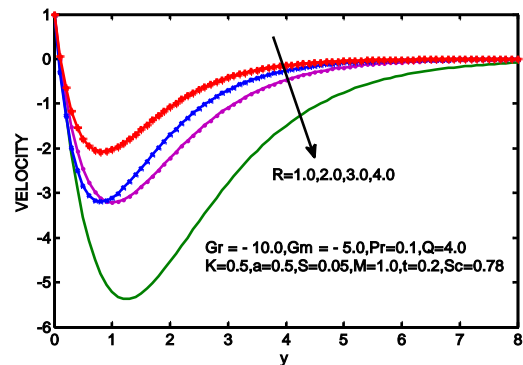


Figure 17. Velocity profiles for different values of R



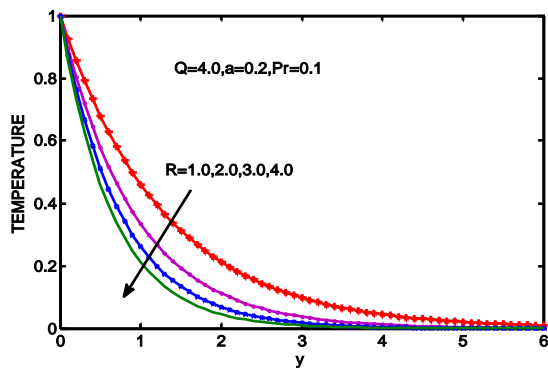


Figure 18. Temperature profiles for different values of R

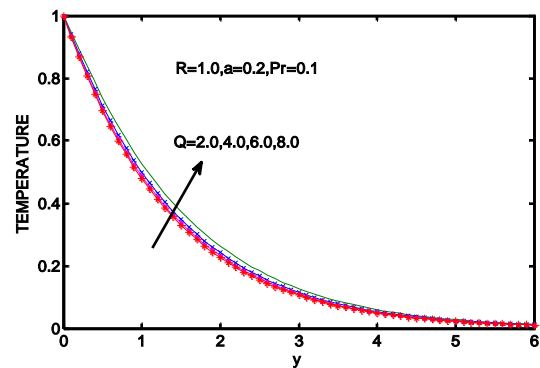


Figure 19. Temperature profiles for different values of Q

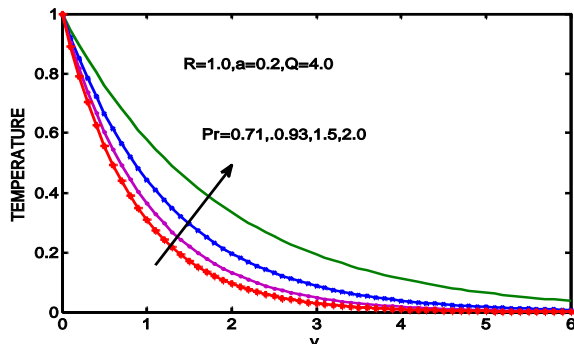


Figure 20. Temperature profiles for different values of Pr

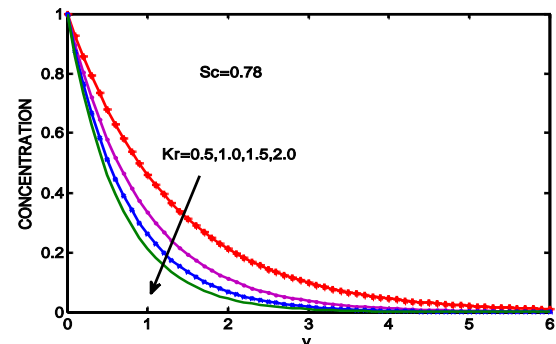


Figure 21. Concentration profiles for different values of Kr

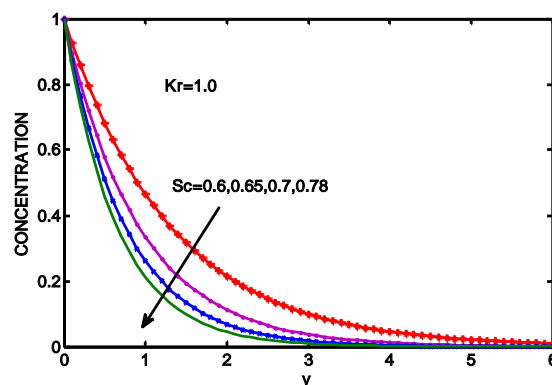


Figure 22. Concentration profiles for different values of Sc

## REFERENCES

1. Chamkha A J (2004): Unsteady MHD convective heat and mass transfer past a semi-vertical permeable moving plate with heat absorption. *Int. J. Eng., Sci.*, 42: pp. 217-230.
2. Deka R Das U N and Soundalgekar V M (1994): Effect of mass transfer on flow past impulsively started infinite vertical plate with a constant heat flux and chemical reaction. *FORSCHUNG IM INGENIEURWESEN*; 60: pp. 284-287.
3. Gireesh Kumar J and Satyanarayana P V (2011): Mass transfer effects on MHD unsteady free convective Walter's memory flow with constant suction and heat sink, *Int. J. of Appl. Math and Mech.* 7 (19): pp. 97-109.
4. Kesavaiah D Ch, Satyanarayana P V and Venkataramana S (2011): Effects of the chemical reaction and radiation absorption on an unsteady MHD convective heat and mass transfer flow past a semi-infinite vertical permeable moving plate embedded in a porous medium with heat source and suction *Int. J. of Appl. Math and Mech.* 7 (1): pp. 52-69.
5. D.Raju (2017): Heat and Mass Transfer to Unsteady MHD Viscoelastic Slip Flow through a Porous Medium with Chemical Reaction. *Int. J. on Future Revolution in Computer Science & Communication Engineering.* 3 (11): pp. 7-16.
6. Muthucumaraswamy R and Ganesan P (2001): Effect of the chemical reaction and injection on flow characteristics in an unsteady upward motion of an isothermal plate, *J. App., Mech., Tech., Phys.*, 42: pp. 665-671.
7. Raptis A (1998): Radiation and free convection flow through a porous medium, *Int., Comm., Heat Mass Transfer*, 25: pp. 289-295.

8. Soundalgekar V M and Patti M R (1980): Stokes problem for a vertical plate with constant heat flux. *Astrophys., Space Sci.*, 70: pp. 179-182
9. Sudheer Babu and M and Satyanarayana P V (2009): Effects of the chemical reaction and radiation absorption on free convection flow through porous medium with variable suction in the presence of uniform magnetic field, *J.P. Journal of Heat and mass transfer*, 3: pp. 219-234
10. Q. Li and Y.M. Xuan (2002): Convective heat transfer and flow characteristics of Cu-water nanofluid, *Sci. China Ser. E Technol. Sci.* 45 (4), pp. 408–416.
11. X.X. Hu, Y.P. Zhang (2002): Novel insight and numerical analysis of convective heat transfer enhancement with microencapsulated phase change material slurries: laminar flow in a circular tube with constant heat flux, *Int. J. Heat Mass Transfer* 45 (15), pp. 3163–3172.
12. D. Angirasa (2002): Experimental investigation of forced convection heat transfer augmentation with metallic fibrous materials, *Int. J. Heat Mass Transfer* 45 (4), pp. 919– 922.
13. J.R. Barbosa G.F. Hewitt G. Konig S.M (2002): Richardson, Liquid entrainment, droplet concentration and pressure gradient at the onset of annular flow in a vertical pipe, *Int. J. Multiphase Flow* 28 (6), pp. 943–961.
14. K. Chakrabandhu and R.K. Singh (2002): Fluid-to-particle heat transfer coefficients for continuous flow of suspensions in coiled tube and straight tube with bends, *Lebensm. -Wissens. Technol. Sci. Technol.* 35 (5), pp. 420–435.
15. S.Y. Jeong and S. Garimella (2002): Falling-film and droplet mode heat and mass transfer in a horizontal tube LiBr/water absorber, *Int. J. Heat Mass Transfer* 45 (7) (2002) 1445– 1458.
16. D. Kim (2002): Improved convective heat transfer correlations for two-phase two-component pipe flow, *KSME J.* 16 (3), pp. 403–422.
17. D. Kim and A.J. Ghajar (2002): Heat transfer measurements and correlations for air-water flow of different flow patterns in a horizontal pipe, *Exper. Therm. Fluid Sci.* 25 (8), pp. 659–676.
18. A.K. Kolar and R. Sundaresan (2002): Heat transfer characteristics at an axial tube in a circulating fluidized bed riser, *Int. J. Therm. Sci.* 41 (7), pp. 673–681.
19. M.M. Kaminski (2002): On probabilistic viscous incompressible flow of some composite fluids, *Computat. Mech.* 28 (6), pp. 505–517.
20. S. Syrjala (2002): Accurate prediction of friction factor and Nusselt number for some duct flows of power-law non-Newtonian fluids, *Numer. Heat Transfer Pt. A-Appl.* 41, (1), pp. 89–100.
21. U.C.S. Nascimento, E.N. Macedo and J.N.N. Quaresma (2002): Thermal entry region analysis through the finite integral transform technique in laminar flow of Bingham fluids within concentric annular ducts, *Int. J. Heat Mass Transfer* 45 (4), pp. 923–929.
22. R.M. Manglik and P. Fang (2002): Thermal processing of viscous non-Newtonian fluids in annular ducts: effects of powerlaw rheology, duct eccentricity, and thermal boundary conditions, *Int. J. Heat Mass Transfer* 45 (4), pp. 803– 814.
23. N. Luna, F. Mendez and C. Trevino (2002): Conjugated heat transfer in circular ducts with a power-law laminar convection fluid flow, *Int. J. Heat Mass Transfer* 45 (3), pp. 655–666.
24. P.M. Coelho, F.T. Pinho, P.J. Oliveira (2002): Fully developed forced convection of the Phan-Thien-Tanner fluid in ducts with a constant wall temperature, *Int. J. Heat Mass Transfer* 45 (7), pp. 1413–1423.
25. H. Struchtrup (2002): Heat transfer in the transition regime: solution of boundary value problems for Grad moment equations via kinetic schemes, *Phys. Rev. E*, p.1204.
26. Q.H. Sun, I.D. Boyd and G.V. Candler (2002): Numerical simulation of gas flow over micro scale airfoils, *J. Thermophys. Heat Transfer*, 16 (2), pp. 171–179.
27. C.E. Siewert (2002): On computing the Chapman–Enskog functions for viscosity and heat transfer and the Burnett functions, *J. Quantitative Spectrosc. Radiat. Transfer.* 74, (6), pp. 789–796.
28. A.D. Polyandin and A.I. Zhurov (2002): Methods of generalized and functional separation of variables in hydrodynamic and heat- and mass-transfer equations, *Theoret. Foundat. Chem. Eng.* 36 (3), pp. 201–213.
29. D. Pal and H. Mondal (2009): Influence of temperature-dependent viscosity and thermal radiation on MHD forced convection over a non-isothermal wedge, *Applied Mathematics and Computation.*, 212, pp. 194–208.
30. P. Ram, A. Bhandari and K. Sharma (2010): Effect of magnetic field-dependent viscosity on revolving ferrofluid, *Journal of Magnetism and Magnetic Materials.*, 322 (21), pp. 3476–3480.
31. M.A. Hossain and I. Pop (1997): Radiation effect on Darcy free convection in boundary layer flow along an inclined surface placed in porous media, *Heat and Mass Transfer.*, 32 (4), pp. 223–227.
32. Cogly A C, Vincentry W C and Gilles S E (1968): A Differential approximation for radiative transfer in a non-gray gas near equilibrium, *AIAA Journal*, 6: pp. 551-555
33. Beard DM and Walters K (1964): Elastico-viscous boundary layer flows, two dimensional flows near a stagnation point. *Proc. Camb. Phil. Soc.* 60: pp. 667-674.

**Source of support: UGC, India, Conflict of interest: None Declared.**

**[Copy right © 2017. This is an Open Access article distributed under the terms of the International Journal of Mathematical Archive (IJMA), which permits unrestricted use, distribution, and reproduction in any medium, provided the original work is properly cited.]**